PHYSICAL REVIEW B **88**, 241301(R) (2013)

Thermally excited multiband conduction in $LaAlO_3/SrTiO_3$ heterostructures exhibiting magnetic scattering

V. K. Guduru,[1,*] A. McCollam,[1] A. Jost,[1] S. Wenderich,[2] H. Hilgenkamp,[2] J. C. Maan,[1] A. Brinkman,[2] and U. Zeitler[1,†]
[1] *High Field Magnet Laboratory and Institute for Molecules and Materials, Radboud University Nijmegen, 6525 ED Nijmegen, The Netherlands*
[2] *Faculty of Science and Technology and MESA+ Institute for Nanotechnology, University of Twente, 7500 AE Enschede, The Netherlands*
(Received 7 October 2013; revised manuscript received 7 November 2013; published 10 December 2013)

Magnetotransport measurements of charge carriers at the interface of a $LaAlO_3/SrTiO_3$ heterostructure with 26 unit cells of $LaAlO_3$ show Hall resistance and magnetoresistance which at low and high temperatures is described by a single channel of electronlike charge carriers. At intermediate temperatures, we observe nonlinear Hall resistance and positive magnetoresistance, establishing the presence of at least two electronlike channels with significantly different mobilities and carrier concentrations. These channels are separated by 6 meV in energy and their temperature-dependent occupation and mobilities are responsible for the observed transport properties of the interface. We observe that one of the channels has a mobility that decreases with decreasing temperature, consistent with magnetic scattering in this channel.

DOI: 10.1103/PhysRevB.88.241301 PACS number(s): 73.20.−r, 73.50.Fq, 73.50.Pz

The study of fundamental physical properties and potential applications of complex oxide heterostructures is a rapidly developing field of research.[1–3] Interest is largely focused on the conducting interface between two band-insulating perovskite oxides $SrTiO_3$ (STO) and $LaAlO_3$ (LAO),[4] which exhibits properties such as superconductivity,[5] magnetism,[6–11] and tunable switching of high mobility interface conductivity.[12–14] Although several mechanisms[15–18] are proposed to be responsible for the interface conductivity, the exact origin and nature of the charge carriers at the interface is still under debate. The major difficulty in achieving consensus about the intrinsic electronic nature of the interfaces is due to the fact that their properties strongly depend on external factors such as the growth conditions of the LAO layer,[6] LAO layer thickness,[19,20] and the configuration of the heterostructures.[21,22] In order to realize the full potential of LAO/STO heterostructures in technological applications,[2,3] the fundamental physical nature of the interface conductivity has to be understood thoroughly.

In this work we study the interface electronic structure of one specific type of LAO/STO heterostructure, which exhibits magnetic signatures.[6] We have performed transport experiments with the magnetic field oriented perpendicular and parallel to the interface, and measured the Hall resistance and sheet resistance in a wide temperature range and at high magnetic fields compared to previous magnetotransport reports.[6,7,23–26] We observed a strong, temperature-dependent, nonlinear Hall resistance accompanied by a large positive magnetoresistance (MR) at intermediate temperatures, and a negative MR at low temperatures.[27] We quantitatively analyze our data using a simple two-carrier model, considering two electronlike conduction channels with different densities and mobilities. Our interpretation is in line with recent observations that two-channel (electronlike) conduction can be realized in similar LAO/STO heterostructures by means of UV illumination on the surface of a sample at low temperature.[14] Furthermore, we show that the negative MR[6] at low temperatures is not a result of two-band conduction alone. Rather, we observe that one of the channels has a mobility that decreases with decreasing temperature, consistent with the previously suggested[6] magnetic scattering scenario in this channel.

The sample used for our measurements was grown by pulsed laser deposition using a single-crystalline $LaAlO_3$ target. The 10 nm (26 unit cells) LAO film was deposited on a 5 mm × 5 mm TiO_2-terminated single crystal STO [001] substrate,[28] at a substrate temperature of 850 °C and an oxygen pressure of 2×10^{-3} mbar. The growth of the LAO film was monitored using *in situ* reflection high-energy electron diffraction, indicating that layer-by-layer growth of individual LAO unit cells (uc) is preserved up to 26 uc. After the growth, the sample was cooled to room temperature with the oxygen pressure remaining at 2×10^{-3} mbar.

The sample was mounted on a ceramic chip carrier and electrical contacts were made by ultrasonically bonding aluminum wires. The sample resistance was measured with the contacts as schematically depicted in the inset of Fig. 1: We denote the resistance as $R_{ij,kl}$, where current is passed through the contacts i and j, and the voltage drop is measured between k and l. For a homogeneous sample, the sheet resistance R_s is calculated from $R_{34,56}$ using the relation $R_s = 1.5 \times R_{34,56}$. We have determined the numeric ratio between R_s and $R_{34,56}$ by van der Pauw measurements on different contact configurations where we find similar values for R_s.

The magnetotransport measurements were performed in a temperature controlled ^{4}He flow cryostat and in a pumped ^{3}He system at magnetic fields up to 30 T. The sheet resistance and Hall resistance ($R_{xy} = R_{34,12}$) were measured for both positive and negative magnetic field directions, using a standard, low-frequency lock-in technique with an excitation current of 1 μA. In order to exclude admixtures of R_s in R_{xy} or vice versa we always show the antisymmetrized Hall resistance data and symmetrized sheet resistance data in the remainder of this Rapid Communication. The results we report here have been reproduced on several similar samples.

The measured sheet resistance R_s is shown as a function of temperature between 2 and 300 K in Fig. 1. Three distinct regimes can be observed in $R_s(T)$: In region I, from 2 to

 ©2013 American Physical Society

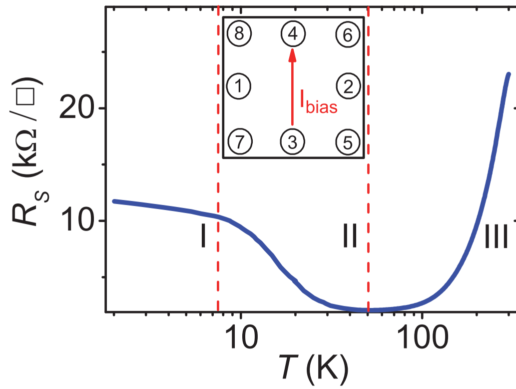

FIG. 1. (Color online) The sheet resistance R_s of the sample as a function of temperature (on a logarithmic scale) between 2 and 300 K, separated by dashed lines in three regimes. The inset shows the schematic top view of the sample, with the contact configuration indicated as circles and the bias current I_{bias} with an arrow.

7.5 K, the sheet resistance decreases logarithmically with an increase in temperature up to 7.5 K, which is attributed to the Kondo effect originating from the scattering of mobile carriers off localized magnetic moments[6] (our measurements do not extend to low enough temperature to see saturation of this effect); in region II, from 7.5 to 50 K, a further increase of temperature leads to a sharp decrease of resistance with a minimum value around 50 K; in region III, above 50 K, the sample resistance increases monotonically with temperature, which can be attributed to electron-phonon scattering.

Figures 2(a) and 2(b) show the Hall resistance and sheet resistance, respectively, in the magnetic field applied perpendicular to the LAO/STO interface, for temperatures between 0.3 (region I) and 65 K (region III). At low temperatures, below 7.5 K, the Hall resistance is linear and independent of temperature, and the sheet resistance decreases as a function of magnetic field, resulting in a strong negative MR. At intermediate temperatures, from 7.5 to 50 K, the Hall resistance is strikingly nonlinear and the sheet resistance increases strongly as a function of magnetic field, resulting in a large positive MR. At high temperatures, above 50 K, the Hall resistance is linear and the sheet resistance increases slightly as a function of magnetic field, resulting in a negligible positive MR. We also observed a similar nonlinear Hall resistance accompanied by a large positive MR, in several other LAO/STO samples with different thicknesses (5, 10, 15, and 20 unit cells) of LAO film at low temperature (4.2 K).

Observations of a temperature-dependent MR (positive and/or negative) and (nonlinear) Hall resistance have been well documented in many different materials; for example, in doped conventional semiconductors such as n-type Ge, GaAs, InSb, and Mn doped GaAs,[29–32] in noble metals doped with transition elements, such as Au doped with Co,[33] and in (magnetic) semiconductor heterostructures (AlGaAs/GaAs, InMnAs/GaAlSb),[34,35] as well as in perovskite oxide heterostructures ($LaTiO_3/SrTiO_3$, $LaVO_3/SrTiO_3$, $LaNiO_3/SrTiO_3$).[36–38] A temperature-dependent crossover from negative to positive MR has also been observed in doped semiconductors (In doped CdS)[39] and in magnetic semiconductor heterostructures (InMnAs/GaAlSb).[32,35] The general consensus is that positive MR and nonlinear Hall resistance arise due to the contribution to transport of two parallel channels of charge carriers with different mobilities. The change in resistance is attributed to the change of electron distribution and mobility in these two channels, caused by the temperature or magnetic field. Negative MR is largely attributed to scattering of conduction charge carriers with localized magnetic moments: The external magnetic field reduces this scattering and results in a decrease of resistance.[39]

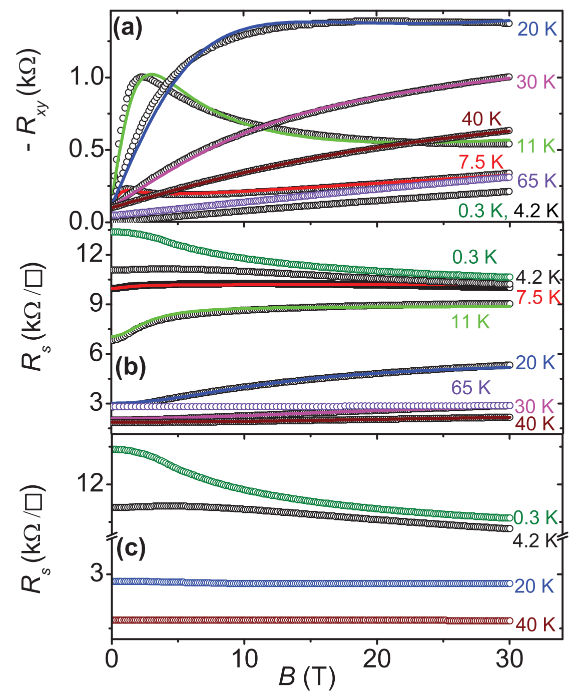

FIG. 2. (Color online) (a) Hall resistance R_{xy} and (b) sheet resistance R_s with the magnetic field oriented perpendicular to the LAO/STO interface for temperatures between 0.3 and 65 K, shown as open circles. Solid lines in (a) and (b) are the results obtained after simultaneously fitting the R_{xy} and R_s data using a simple two-carrier model. The R_{xy} curves are offset vertically for clarity. (c) Sheet resistance R_s for the applied magnetic field oriented parallel to the LAO/STO interface for temperatures between 0.3 and 40 K, shown as open circles. R_s axis is cut between 4 and 10 kΩ.

Figure 2(c) shows the sheet resistance data for the applied magnetic field orientation parallel to the LAO/STO interface, for temperatures between 0.3 (region I) and 40 K (region II). At low temperatures, the sheet resistance decreases as a function of magnetic field, resulting in a strong negative MR. The MR below 4.2 K is independent of the field orientation, at odds with an interpretation in terms of weak localization, and consistent with electron spin scattering off localized magnetic moments.[6] The decrease in magnitude of the negative MR with increased temperature can be attributed to the delocalization of magnetic moments by thermal excitation at higher temperatures.[23,40] At intermediate temperatures, the sheet resistance is almost field independent.

The linear Hall resistance below 7.5 (region I) and above 50 K (region III) can be described using the conventional single-carrier model. The carrier concentration $[n_s = B/R_{xy}e]$ and mobility $[\mu = 1/R_s(0)en_s]$ are extracted from the slope of the linear Hall resistance data and zero field sheet resistance

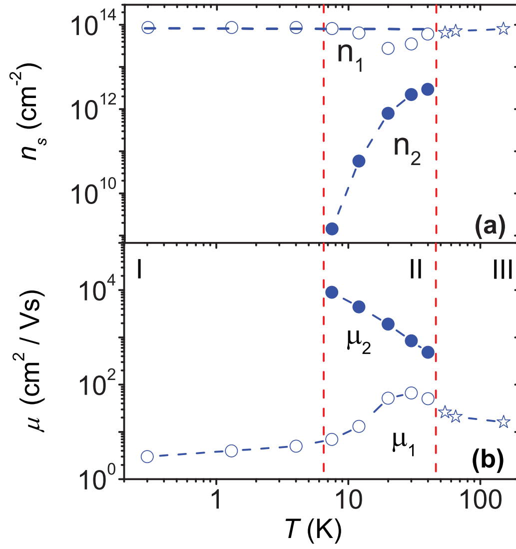

FIG. 3. (Color online) The temperature dependence of sheet carrier density n_s and mobility μ obtained from the analysis of experimental data in Figs. 2(a) and 2(b). (a) The sheet carrier density n_s for regions I and II are shown as open circles (n_1), filled circles (n_2), and for region III are shown as stars. (b) The carrier mobility μ for regions I and II is shown as open circles (μ_1), filled circles (μ_2), and for region III is shown as stars. The connecting dashed lines between the data points are guides to the eye.

$R_s(0)$ with e as the electronic charge. The values obtained for n_s and μ by the single-carrier model are shown in Figs. 3(a) and 3(b).

In contrast, the nonlinear Hall resistance and positive MR between 7.5 and 50 K (region II) cannot be explained within a single-carrier model, but rather suggest a multichannel system. A similar nonlinear Hall resistance and positive MR were observed previously in $LaTiO_3/SrTiO_3$,[38] and explained in terms of two-channel conduction from electronic bands with different mobilities, $\mu_{1,2}$, and carrier densities, $n_{1,2}$. We use similar two-electron-band expressions,[41]

$$R_{xy}(B) = \frac{B}{e}\frac{\left(n_1\mu_1^2 + n_2\mu_2^2\right) + (\mu_1\mu_2 B)^2(n_1+n_2)}{(n_1\mu_1+n_2\mu_2)^2 + (\mu_1\mu_2 B)^2(n_1+n_2)^2}, \quad (1)$$

$$R_s(B) = R_s(0)\left[1 + \frac{(n_1\mu_1 n_2\mu_2(\mu_1-\mu_2)^2B^2)}{(n_1\mu_1+n_2\mu_2)^2 + ((n_1+n_2)\mu_1\mu_2 B)^2}\right], \quad (2)$$

to model our nonlinear Hall resistance $R_{xy}(B)$ and sheet resistance $R_s(B)$ data as a function of magnetic field.

In this expression, we take n_1,μ_1 to be the carrier density and mobility of the existing electron band at low temperatures and n_2,μ_2 are the carrier density and mobility of the thermally activated second electron band. For low magnetic fields, where $\mu_1 B,\mu_2 B \ll 1$, $R_{xy}(B)$ shows B-linear behavior, and $R_s(B)$ shows quadratic dependency on B. For high magnetic fields, where $\mu_1 B,\mu_2 B \gg 1$, $R_{xy}(B)$ shows B-linear behavior, and $R_s(B)$ saturates. In the field region where $\mu_2 B \simeq 1$ or $\mu_1 B \simeq 1$, $R_{xy}(B)$ shows strongly nonlinear behavior.

Fits of the Hall resistance and sheet resistance to this two-band model are shown in Figs. 2(a) and 2(b) as solid lines. The nonlinear Hall resistance $R_{xy}(B)$ and sheet resistance $R_s(B)$ at each temperature were fitted simultaneously, using n_1,n_2 and μ_1,μ_2 as fit parameters. The fits are in good agreement with the experimental data and the model is able to nicely reproduce the details of the magnetotransport [$R_{xy}(B)$ and $R_s(B)$] in the temperature region between 7.5 to 50 K, where the data cannot be described within a single carrier model.

The results of our analysis of the magnetotransport data in the three temperature regions are shown in Fig. 3, with the obtained values for the fit parameters n_1,n_2 in Fig. 3(a) and μ_1,μ_2 in Fig. 3(b).

For temperatures below 7.5 K (region I), transport is dominated by a low mobility electron band with a temperature-independent linear Hall resistance yielding a constant, high, sheet density of $n_1 = 8.7 \times 10^{13}$ cm^{-2}. The mobility of electrons in this band increases from $\mu_1 = 3$ cm^2/V s to 5 cm^2/V s with an increase in temperature from 0.3 to 4.2 K. This temperature-dependent mobility can be attributed to magnetic scattering which also explains the observed negative MR.[6]

For temperatures between 7.5 and 50 K (region II), electrons are thermally activated into a second electron band (n_2,μ_2) in addition to the existing low mobility electron band (n_1,μ_1). The carrier density n_1 in the low mobility electron band stays almost temperature independent, while the mobility μ_1 increases by about an order of magnitude from 7 cm^2/V s to 50 cm^2/V s. The carrier density n_2 in the second electron band shows a strong temperature dependence and increases by a few orders of magnitude from 1.4×10^9 cm^{-2} to 2.9×10^{12} cm^{-2}, the mobility μ_2 decreases by an order of magnitude from 8×10^3 cm^2/V s to 4×10^2 cm^2/V s. The decrease in mobility of μ_2 as the temperature increases is likely to be the result of increased electron-phonon scattering. At low temperature μ_1 is dominated by magnetic scattering, which is expected to decrease with increasing temperature leading to the observed increase in μ_1. As the temperature is further increased, electron-phonon scattering also begins to strongly affect the lower energy conduction channel, so that μ_1 reaches a maximum (at $\sim$30 K) and then decreases at higher temperatures.

This thermal activation of electrons into a second energetically higher channel is visualized in Fig. 4(a). The activation energy of carriers ε is related to the concentration in the second electron channel by the Arrhenius relation $n_2 \propto \exp(-\varepsilon/k_B T)$, where k_B is the Boltzmann constant and T is temperature. The linear slope of $\ln(n_2)$ versus $1/T$ gives $\varepsilon = 6$ meV. For temperatures above 50 K (region III), the

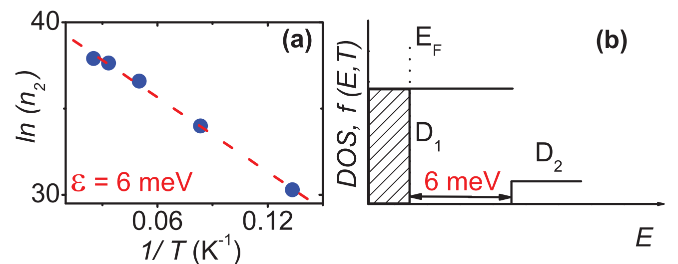

FIG. 4. (Color online) (a) Arrhenius plot of the thermally excited carrier density n_2. The slope of the dashed line gives $\varepsilon = 6$ meV. (b) Schematic representation of the 2D level structure with constant density of states for the two parallel electronlike conduction channels at the interface. At $T = 0$ K, the level D_1 is occupied up to the Fermi energy E_F (dotted line); at $T = 60$ K, broadening (6 meV) of the Fermi function results in the occupation of level D_2.

mobilities of the two electron channels become comparable and the two channels no longer give distinguishable contributions to the transport (see expressions 1 and 2). The *total* carrier concentration and mobility are then obtained from a single band calculation. The total carrier concentration remains temperature independent and the average mobility further decreases with increasing temperature.

We explain our results by tentatively considering two simplified interface electronic states with a constant two-dimensional (2D) density of states D_1 and D_2 as schematically depicted in Fig. 4(b). The oxygen vacancies in STO (each oxygen vacancy donates two free electrons) and/or the electronic reconstruction (half an electron transfer from LAO to STO) give a reservoir of charge carriers at the interface, which includes both localized and mobile carriers. At finite (low) temperature (region I), the charge carriers are present in a lower energy level (D_1) which has a low mobility (μ_1) and high electron density (n_1). These carriers are responsible for the observed Kondo-type behavior (i.e., logarithmic increase of sheet resistance accompanied by the decrease of carrier mobility for decreasing temperature down to 0.3 K), negative MR, and linear Hall resistance. On increasing the temperature through region II, broadening of the Fermi function results in the thermal excitation of charge carriers into a higher energy level (D_2) separated from the lower level by 6 meV, which has a high mobility (μ_2) and low electron density (n_2). Both the low and high mobility bands contribute to the transport in region II and are responsible for the observed large, positive MR and nonlinear Hall resistance. When the temperature is further increased above 50 K (region III), the mobilities of these two conduction channels become similar. As a result we cannot distinguish the two band conduction any longer, which eventually gives rise to a linear Hall resistance and a negligible MR.

Our results and analysis strongly suggest that at least two channels of electronlike carriers at the interface are responsible for the observed transport behavior in these LAO/STO heterostructures exhibiting magnetic scattering, but they do not allow us to determine the exact physical origin of these interface conduction channels. However, from similarities between our results and available information in the literature, we can propose a few possibilities for the origin of the observed electron bands. It has been predicted theoretically[42] and shown experimentally[11] that the magnetism in LAO/STO originates from the t_{2g} band of Ti-3d orbitals, specifically from the energy level formed from d_{xy} orbitals with Ti^{3+} character. This suggests that in our sample the observed energy level (D_1) associated with the low mobility carriers (n_1,μ_1) and responsible for magnetic effects (Kondo effect, negative MR), could originate from these d_{xy} orbitals. The observed energy level (D_2) associated with the high mobility carriers (n_2,μ_2) is separated by 6 meV from the low mobility level in our sample; this activation energy is strikingly similar to values found in earlier observations of carrier activation in $SrTiO_3/LaAlO_3/SrTiO_3$ heterostructures,[21,22] and comparable to La doped $SrTiO_3$.[43] There is evidence from previous work that the higher-energy conduction channel we observe is likely to have primarily $d_{xz/yz}$ character.[44–46] This seems to be a reasonable assumption for our sample, based on the energy separation of the conduction channels and the carrier density involved.[46,47]

We have also performed similar measurements on LAO/STO samples with thinner LAO layers (20, 15, 10, 5 uc of LAO) where we observe two-channel conduction of a high mobility and a low mobility channel, which in contrast to the 26 LAO system, is present down to the lowest temperatures. We interpret this observation by a different energetic alignment of the two channels. This coexistence at low temperature precludes a clear distinction of their individual contribution to magnetotransport as compared to the 26 LAO system where the two channels are well separated.

In summary, we have performed magnetotransport experiments on a magnetic $LaAlO_3/SrTiO_3$ interface, with a 10 nm (26 unit cells) $LaAlO_3$ film, in magnetic fields up to 30 T. Our experimental results show that the low-temperature regime ($T \leqslant 4.2$ K) is dominated by a single charge carrier type with a low mobility, yielding a linear Hall resistance and negative MR. Increasing the temperature above 4.2 K leads to a significant decrease of the resistance, a strong positive MR appears, and the Hall resistance becomes distinctly nonlinear. Our observations are quantitatively explained by thermal excitation of an additional high mobility electron channel situated 6 meV above the low mobility channel.

This work has been performed at the HFML-RU/FOM member of the European Magnetic Field Laboratory (EMFL) and is part of InterPhase programme supported by the Foundation for Fundamental Research on Matter (FOM) with financial support from the Netherlands Organisation for Scientific Research (NWO).

*guduru@science.ru.nl

†u.zeitler@science.ru.nl

[1] H. Y. Hwang, Y. Iwasa, M. Kawasaki, B. Keimer, N. Nagaosa, and Y. Tokura, Nat. Mater. **11**, 103 (2012).

[2] J. Mannhart and D. G. Schlom, Science **327**, 1607 (2010).

[3] E. Assmann, P. Blaha, R. Laskowski, K. Held, S. Okamoto, and G. Sangiovanni, Phys. Rev. Lett. **110**, 078701 (2013).

[4] A. Ohtomo and H. Y. Hwang, Nature (London) **427**, 423 (2004).

[5] N. Reyren, S. Thiel, A. D. Caviglia, L. F. Kourkoutis, G. Hammerl, C. Richter, C. W. Schneider, T. Kopp, A. S. Ruetschi, D. Jaccard, M. Gabay, D. A. Muller, J.-M. Triscone, and J. Mannhart, Science **317**, 1196 (2007).

[6] A. Brinkman, M. Van Zalk, J. Huijben, U. Zeitler, J. C. Maan, W. G. Van der Wiel, G. Rijnders, D. H. A. Blank, and H. Hilgenkamp, Nat. Mater. **6**, 493 (2007).

[7] Ariando, X. Wang, G. Baskaran, Z. Q. Liu, J. Huijben, J. B. Yi, A. Annadi, A. R. Barman, A. Rusydi, S. Dhar, Y. P. Feng, J. Ding, H. Hilgenkamp, and T. Venkatesan, Nat. Commun. **2**, 188 (2011).

[8] D. A. Dikin, M. Mehta, C. W. Bark, C. M. Folkman, C. B. Eom, and V. Chandrasekhar, Phys. Rev. Lett. **107**, 056802 (2011).

[9]L. Li, C. Richter, J. Mannhart, and R. C. Ashoori, Nat. Phys. **7**, 762 (2011).
[10]J. A. Bert, B. Kalisky, C. Bell, M. Kim, Y. Hikita, H. Y. Hwang, and K. A. Moler, Nat. Phys. **7**, 767 (2011).
[11]J.-S. Lee, Y. W. Xie, H. K. Sato, C. Bell, Y. Hikita, H. Y. Hwang, and C.-C. Kao, Nat. Mater. **12**, 703 (2013).
[12]S. Thiel, G. Hammerl, A. Schmehl, C. W. Schneider, and J. Mannhart, Science **313**, 1942 (2006).
[13]A. D. Caviglia, S. Gariglio, N. Reyren, D. Jaccard, T. Schneider, M. Gabay, S. Thiel, G. Hammerl, J. Mannhart, and J.-M. Triscone, Nature (London) **456**, 624 (2008).
[14]V. K. Guduru, A. Granados del Aguila, S. Wenderich, M. K. Kruize, A. McCollam, P. C. M. Christianen, U. Zeitler, A. Brinkman, G. Rijnders, H. Hilgenkamp, and J. C. Maan, Appl. Phys. Lett. **102**, 051604 (2013).
[15]N. Nakagawa, H. Y. Hwang, and D. A. Muller, Nat. Mater. **5**, 204 (2006).
[16]M. Sing, G. Berner, K. Goß, A. Müller, A. Ruff, A. Wetscherek, S. Thiel, J. Mannhart, S. A. Pauli, C. W. Schneider, P. R. Willmott, M. Gorgoi, F. Schäfers, and R. Claessen, Phys. Rev. Lett. **102**, 176805 (2009).
[17]G. Herranz, M. Basletić, M. Bibes, C. Carrétéro, E. Tafra, E. Jacquet, K. Bouzehouane, C. Deranlot, A. Hamzić, J.-M. Broto, A. Barthélémy, and A. Fert, Phys. Rev. Lett. **98**, 216803 (2007).
[18]P. R. Willmott, S. A. Pauli, R. Herger, C. M. Schlepütz, D. Martoccia, B. D. Patterson, B. Delley, R. Clarke, D. Kumah, C. Cionca, and Y. Yacoby, Phys. Rev. Lett. **99**, 155502 (2007).
[19]C. Bell, S. Harashima, Y. Hikita, and H. Y. Hwang, Appl. Phys. Lett. **94**, 222111 (2009).
[20]F. J. Wong, R. V. Chopdekar, and Y. Suzuki, Phys. Rev. B **82**, 165413 (2010).
[21]M. Huijben, G. Koster, M. K. Kruize, S. Wenderich, J. Verbeeck, S. Bals, E. Slooten, B. Shi, H. J. A. Molegraaf, J. E. Kleibeuker, S. van Aert, J. B. Goedkoop, A. Brinkman, D. H. A. Blank, M. S. Golden, G. van Tendeloo, H. Hilgenkamp, and G. Rijnders, Adv. Funct. Mater. **23**, 5240 (2013).
[22]M. Huijben, G. Rijnders, D. H. A. Blank, S. Bals, S. van Aert, J. Verbeeck, G. van Tendeloo, A. Brinkman, and H. Hilgenkamp, Nat. Mater. **5**, 556 (2006).
[23]X. Wang, W. M. Lü, A. Annadi, Z. Q. Liu, K. Gopinadhan, S. Dhar, T. Venkatesan, and Ariando, Phys. Rev. B **84**, 075312 (2011).
[24]T. Hernandez, C. W. Bark, D. A. Felker, C. B. Eom, and M. S. Rzchowski, Phys. Rev. B **85**, 161407 (2012).
[25]C. Bell, S. Harashima, Y. Kozuka, M. Kim, B. G. Kim, Y. Hikita, and H. Y. Hwang, Phys. Rev. Lett. **103**, 226802 (2009).
[26]R. Pentcheva, M. Huijben, K. Otte, W. E. Pickett, J. E. Kleibeuker, J. Huijben, H. Boschker, D. Kockmann, W. Siemons, G. Koster, H. J. W. Zandvliet, G. Rijnders, D. H. A. Blank, H. Hilgenkamp, and A. Brinkman, Phys. Rev. Lett. **104**, 166804 (2010).
[27]V. K. Guduru, A. McCollam, S. Wenderich, M. K. Kruize, A. Brinkman, M. Huijben, G. Koster, D. H. A. Blank, G. Rijnders, H. Hilgenkamp, J. C. Maan, and U. Zeitler, J. Korean Phys. Soc. **63**, 437 (2013).
[28]G. Koster, B. L. Kropman, G. J. H. M. Rijnders, D. H. A. Blank, and H. Rogalla, Appl. Phys. Lett. **73**, 2920 (1998).
[29]J. F. Woods and C. Y. Chen, Phys. Rev. **135**, A1462 (1964).
[30]Y. Katayama and S. Tanaka, Phys. Rev. **153**, 873 (1967).
[31]L. Halbo and R. J. Sladek, Phys. Rev. **173**, 794 (1968).
[32]F. Matsukura, H. Ohno, A. Shen, and Y. Sugawara, Phys. Rev. B **57**, R2037 (1998).
[33]A. N. Gerritsen, Physica **25**, 489 (1959).
[34]H. van Houten, J. G. Williamson, M. E. I. Broekaart, C. T. Foxon, and J. J. Harris, Phys. Rev. B **37**, 2756 (1988).
[35]A. Oiwa, A. Endo, S. Katsumoto, Y. Iye, H. Ohno, and H. Munekata, Phys. Rev. B **59**, 5826 (1999).
[36]Y. Hotta, T. Susaki, and H. Y. Hwang, Phys. Rev. Lett. **99**, 236805 (2007).
[37]R. Scherwitzl, S. Gariglio, M. Gabay, P. Zubko, M. Gibert, and J.-M. Triscone, Phys. Rev. Lett. **106**, 246403 (2011).
[38]J. S. Kim, S. S. A. Seo, M. F. Chisholm, R. K. Kremer, H. U. Habermeier, B. Keimer, and H. N. Lee, Phys. Rev. B **82**, 201407 (2010).
[39]R. P. Khosla and J. R. Fischer, Phys. Rev. B **2**, 4084 (1970).
[40]M. Lee, J. R. Williams, S. Zhang, C. D. Frisbie, and D. Goldhaber-Gordon, Phys. Rev. Lett. **107**, 256601 (2011).
[41]N. W. Ashcroft and N. D. Mermin, *Solid State Physics* (Harcourt Brace College Publishers, Fort Worth, Texas, 1976), p. 240.
[42]R. Pentcheva and W. E. Pickett, Phys. Rev. Lett. **99**, 016802 (2007).
[43]T. Okuda, K. Nakanishi, S. Miyasaka, and Y. Tokura, Phys. Rev. B **63**, 113104 (2001).
[44]M. Salluzzo, J. C. Cezar, N. B. Brookes, V. Bisogni, G. M. De Luca, C. Richter, S. Thiel, J. Mannhart, M. Huijben, A. Brinkman, G. Rijnders, and G. Ghiringhelli, Phys. Rev. Lett. **102**, 166804 (2009).
[45]G. Berner, M. Sing, H. Fujiwara, A. Yasui, Y. Saitoh, A. Yamasaki, Y. Nishitani, A. Sekiyama, N. Pavlenko, T. Kopp, C. Richter, J. Mannhart, S. Suga, and R. Claessen, Phys. Rev. Lett. **110**, 247601 (2013).
[46]G. Khalsa and A. H. MacDonald, Phys. Rev. B **86**, 125121 (2012).
[47]L. W. van Heeringen, G. A. de Wijs, A. McCollam, J. C. Maan, and A. Fasolino, Phys. Rev. B **88**, 205140 (2013).